Nanofabrication (2024) 9
https://doi.org/10.37819/nanofab.9.1798

RESEARCH ARTICLE

Process optimization for biogenesis of silver nanoparticles from *Aspergillus flavus* GGRK1 culture filtrate: Characterization and Its antibacterial efficacy

Divya Naini[a#], Guddu Kumar Gupta[b#], Gaurav Rawat[b], Sonia Kapoor[a], Rajeev Kumar Kapoor[b*]
[a]Department of Biotechnology, UIET, Maharshi Dayanand University, Rohtak-124001, Haryana, India
[b]Enzyme and Fermentation Technology Laboratory, Department of Microbiology, Maharshi Dayanand University, Rohtak-124001, Haryana, India
***Corresponding author's Email**: patent.agent.biotech@gmail.com

Equal first author

Abstract

The cell-free culture filtrate (CF) of *Aspergillus flavus* GGRK1 could mediate the synthesis of silver nanoparticles using silver nitrate. Extracellular extract of *Aspergillus flavus* GGRK1 was a significant reductant for the reduction of silver nanoparticles due to presence of metabolites or other bioactive compounds. After the reduction of Ag (I) ions to Ag by the fungal CF, a dark brown color was obtained which indicated the biosynthesis of AgNPs. The maximum AgNPs were synthesized at the CCD-optimized condition of $AgNO_3$ conc. of 4.189 mM, CFC 0.905 mL, and reaction time 8.17 h. The biosynthesized AgNPs had a zeta size of 119.4 nm diameter. The FTIR study revealed the significant efficacy of functional groups associated with the biosynthesized AgNPs. Additionally, the XRD study revealed a crystalline nature of biosynthesized AgNPs along very good correlation with FCC lattice. The biosynthesized nanoparticles showed significant antibacterial activity against gram-positive and gram-negative bacteria. As a result, the maximum ZOI was obtained at 150 µl/ml against all the tested organisms such as *B. subtilis* MTCC 121, *S. aureus* MTCC 96, *E coli* MTCC 443 and *P. aeruginosa* MTCC 424 with 18 mm, 20 mm, 14 mm, and 18 mm, respectively.

Keywords: Silver nanoparticles; Response surface methodology; Biosynthesis optimization; Greener synthesis; Antibacterial efficacy

Article history:

Received: 15-Sep-2023
Revised: 21-Nov-2023
Accepted: 14-Jan-2024

Introduction

The scientific field of nanotechnology works with a range of nanostructures used in the biomedical, biosensor manufacturing, environment, and agriculture sectors. Nanoscale particles with sizes between 1 and 100 nm or smaller are known as nanoparticles (Shinde et al., 2022). Metal nanoparticles such as silver, copper, titanium, and others are very fine and strong particles with applications in a variety of fields such as medicine, drug delivery, bio labeling, nanocomposites, antimicrobial substances, intercalating material for electrical items, and acting as catalysts in chemical reactions. With decreasing size, nanoparticles exhibit a larger surface-to-volume ratio. Catalytic reactivity and other related qualities, such as antibacterial activity, are related to specific surface area (Ifijen et al., 2022). Several techniques can be used to produce nanoparticles. The most used processes for creating nanoparticles are chemical ones. Certain chemical techniques, however, cannot avoid using harmful compounds in the synthesis pathway. Since metal nanoparticles are frequently used in regions where people meet them, there is an increasing need to create ecologically safe nanoparticle synthesis techniques that don't include hazardous chemicals.
As potential environmentally acceptable alternatives to chemical and physical approaches, biological methods for nanoparticle manufacturing have been proposed (Singh et al., 2015). These methods use microbes, enzymes, plants,

or plant extracts. The creation of nanoparticles has reportedly been carried out using microorganisms such as bacteria (Lee et al., 2011), fungi, actinomycetes (Ma et al., 2017), and even higher plant leaves (Wei et al., 2020).
Filamentous fungi have advantages over the other microbes for the biogenic synthesis of nanoparticles because of their high secretion of extracellular enzymes, and metabolites, higher growth rates and low-cost requirements for production procedures. In addition, biogenic synthesis of nanoparticles using fungi gives high monodispersity and greater stability as compared to other microorganisms (Chauhan et al., 2023; Dhillon et al., 2012; Kapoor et al., 2021; Khandel & Shahi, 2018). Farrag et al. in 2020 reported that *A. niger* was used for the biosynthesis of silver nanoparticles and it has significant biological activity (Farrag et al., 2020). Similarly, another fungus *A. fumigatus* was reported for the biosynthesis of silver nanoparticles (Bhainsa & D'Souza, 2006). As a result, several fungal species have been utilized for the biogenic synthesis of silver nanoparticles, some of which include *penicillium* (Nayak et al., 2011), *Fusarium oxysporum* (Mostafa, 2017) and some species of *Aspergillus* (Elshafei et al., 2021; Sheikh & Awad, 2022; Sulaiman et al., 2015).
Because of its size-dependent property, silver nanoparticles (AgNPs) are one of the most extensively used nanoparticles. The biological and physical parameters that affect this green synthesis of $AgNO_3$ include the solvent, medium, temperature, light, pressure, and pH conditions (Wei et al., 2020). This property reveals a wide range of applications, including the development of biological products, drug delivery systems, battling cancer, antimicrobial efficacy, and water purification (Hulkoti & Taranath, 2014). Although silver is poisonous to mammals, it has been shown to be non-toxic to human cells at low concentrations (Singh et al., 2018), leading to its widespread usage in in-vitro and in-vivo research. However, research on the synthesis and characterization of AgNPs has been significantly increased. AgNPs of various sizes and shapes have varied plasmon resonance bands, which results in a variety of colored suspensions. Numerous chemically mediated methods of producing high-yield nanoparticles, such as spherical AgNPs synthesis and triangular AgNPs production (Mansouri & Ghader, 2009), have been reported by numerous researchers since high-yield nanoparticle production and size analysis have become a critical focus of demanding research. Furthermore, several kinds of literature have been found and published related to AgNP synthesis, largely to boost yield and improve product stability, particularly in bulk production. Stirring time, for example, was discovered to have an effect on surface plasma resonance (SPR) (Balavandy et al., 2014).
In the present study, conventional and statistical optimization techniques were conducted for maximum production of silver nanoparticles. Furthermore, the biosynthesized AgNPs were characterized through various techniques, and their antibacterial applicability was evaluated.

Materials and methods

Microorganisms and cultural conditions

The fungal culture *Aspergillus flavus* GGRK1 was procured from laboratory number 322, Department of Microbiology, Maharshi Dayanand University, Rohtak. The procured culture was inoculated on Potato dextrose agar (PDA) medium and incubated at 30^0C in a BOD shaker. Subculturing was routinely carried out using PDA slants and stored at 4^0C for further use.

Preparation of cell-free Culture (CFC) supernatant and AgNPs biosynthesis

The spore suspension of 1 mL containing 2.4×10^7 spores/ml was transferred in potato dextrose broth (PDB) medium and incubated at 30^0C in a BOD shaker for 2 days. The biomass was filtered through Whatman No.1 filter paper, and the resulting CFC filtrate was cleared by centrifugation at 10,000 rpm and 40°C for 10 minutes. The cleaned CFC was then utilized to synthesize AgNPs. Briefly, 20 ml reaction mixture containing 2 ml of fungal culture filtrate with 2mM of silver nitrate. All the flasks were incubated at 30^0C in light conditions up to 5 h. the resultant brown color was primarily analyzed using a UV-VIS Spectrophotometer (ELICO Pvt. Ltd. India) at the range of 200-800 nm.

Optimization AgNPs biosynthesis through one factor at a time (OFAT) Approach

Using the OFAT strategy, the optimal operating conditions that had a positive impact on the biosynthesis of AgNPs were optimized. The potential optimum level of factors for the biosynthesis of AgNPs, including suitable growth medium (**Table 1**), CFC volume (0.5 -2.5 mL), effect of silver nitrate concentration (1-5 mM), effect of light and dark conditions, and effect of reaction time (2-10 h) were selected to achieve the suitable conditions. A UV-VIS

Nanofabrication (2024) 9
https://doi.org/10.37819/nanofab.9.1798

Spectrophotometer (ELICO Pvt. Ltd. India) was used to detect absorbance throughout a spectrum range of 200-800 nm.

Table 1. Composition of different media used for screening in Biosynthesis of AgNPs

S. No.	Medium Name	Ingredients	Compositions (g/L)
1	**Potato Dextrose Broth (PDB)**	Infusion from potatoes	200
		Dextrose (Glucose)	
2	**Glucose medium**	Glucose	15
		Ammonium Sulphate	4.0
		K_2HPO_4	1
		$MgSO_4.7H_2O$	0.5
3	**Sucrose medium**	Sucrose	15
		Yeast extract	4
		K_2HPO_4	1
		$MgSO_4.7H_2O$	0.5
4	**Lactose medium**	Lactose	15
		Peptone	4
		K_2HPO_4	1
		$MgSO_4.7H_2O$	0.5

Process optimization of AgNPs biosynthesis through CCD approach using Response Surface Methodology tool

Using Design Expert software (Version 13.0, Stat-Ease, Inc., USA) face-centered central composite experimental design (FCCCD) for RSM was performed to maximize AgNPs biosynthesis. In which the three crucial process input variables namely; (A) $AgNO_3$ concentration, (B) reaction time, and (C) CFC are optimized. The range of process variables are given in **Table 2**. Other process variables such as temperature and light conditions was constant. The experimental matrix with 20 runs was obtained from the FCCCD design (**Table 3**). Statistical analysis was used to assess the developed model, Fisher's F-test, and including analysis of variance (ANOVA). The coefficient of determination, or R^2, was used to describe how well the model equation fits the data. The link between the responses was then depicted using the fitted model as a contour and 3D surface plot. Using the statistical software program Design-Expert 13.0, an optimal combination of the impacts was projected.

Table 2. Levels of input variables for FCCCD optimization

Independent Variables	Levels				
	-α	**-1**	**0**	**+1**	**+α**
Silver Nitrate conc. (mM)	1.0	1.81	3.0	4.19	5.0
CFC (mL)	0.5	0.91	1.5	2.09	2.5
Reaction time (H)	1	2.82	5.50	8.18	10.0

Validation of FCCCD model

By using the ideal values, the model and regression equation were validated. The flask containing the reaction mixture for AgNP synthesis with RSM optimized parameters ($AgNO_3$ conc. of 4.189 mM, CFC 0.905 mL, and

reaction time 8.17 h) and incubated at 30℃ in a BOD incubator in the presence of light. Lastly, to validate the constructed FCCCD model, sets of tests were carried out utilizing the recommended ideal combination.

Characterization of biosynthesized AgNPs

The biosynthesized AgNPs were characterized primarily based on UV-VIS Spectrophotometer (brown color change measured at 200-800 nm) then advanced structural and functional properties such as FTIR, X-ray diffraction, zeta size distribution, and zeta potential analysis were carried out. Furthermore, AgNPs were completely cleaned and scanned using an FT-IR spectrophotometer (Bruker, Germany) in the 400-4000 cm-1 range. The crystallinity nature of biosynthesized AgNPs was determined through an X-ray diffractometer (XRD, Rigaku MiniFlex 600). Additionally, the size distribution and zeta potential were performed at 25°C with the help of a Zeta size analyzer (S90, Malvern, UK). Moreover, the surface morphology and size of biosynthesized AgNPs were analyzed by transmission electron microscope (TEM) (Majeed et al., 2016; Sreenivasa et al., 2021). The polydispersity index was recorded by calculating the average radius of the NPs and the standard deviation with the help of equation

$$p = \sigma/R_{Avg} \quad (1)$$

where σ = standard deviation of the radius of a batch of nanoparticles, p = dispersity, and R_{Avg} = average radius of nanoparticles.

Antibacterial activity of biosynthesized AgNPs

To evaluate the antibacterial activity, a disc diffusion method was performed. The gram-positive (*B. subtilis* MTCC 121 and *S. aureus* MTCC 96) and gram-negative bacteria (*E. coli* MTCC 443 and *P. aeruginosa* MTCC 424) were tested. The inoculums were prepared by inoculating the nutrient broth and incubated at 37℃ in a shaking incubator for 24h. The cultures were diluted with the 0.9% saline solution to obtain 1.5×10^8 CFU/ml. Each culture was spreading with the help of sterilized swabs on MHA plates separately. The ranges of AgNP concentration 50-150 µl/ml were prepared. The sterile discs were dipped into respective AgNP concentrations and then placed on MHA plates. These plates were incubated at 37℃ for 24 hrs. The zone of clearance/inhibition was measured by taking the reading in triplicates.

Results and discussion

Myco-synthesis of AgNPs

To investigate the effectiveness of silver ion reduction and the creation of nanoparticles cell-free culture filtrate was used. After being exposed to $AgNO_3$ at 30℃ temperature and light conditions, the fungal cell filtrate changed colorless to dark brown color within five hours of reacting with Ag^+ ions (**Fig. 1**). The formation of a brown color was definite evidence that the reaction mixture had produced silver nanoparticles. Other researchers who used a fungal system to produce silver nanoparticles reported similar outcomes. The metal nanoparticles' surface plasmon oscillations were excited, which resulted in a change in color. The examination of nanoparticles has proven to benefit greatly from this technique. With a UV-visible spectrophotometer, the absorbance of the filtrate of fungal cells treated with a solution of 1 mM silver nitrate was measured. According to Mie's hypothesis, spherical nanoparticles will have a single SPR band in their absorption spectra, whereas other types of particles may have two or more SPR bands (Thomas et al., 2008).

Nanofabrication (2024) 9
https://doi.org/10.37819/nanofab.9.1798

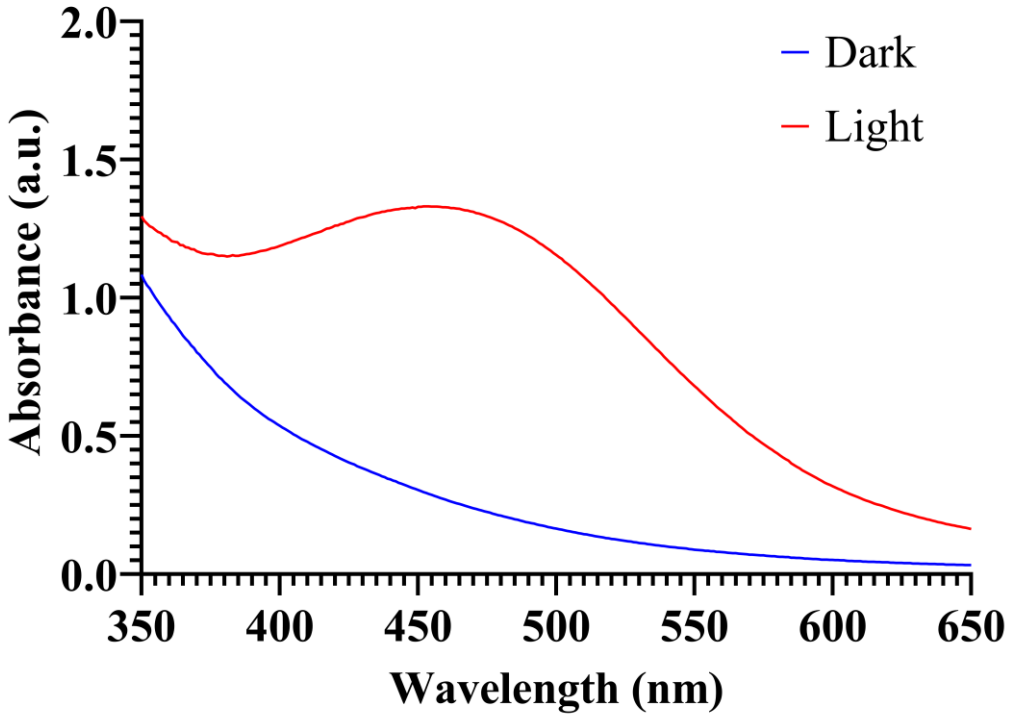

Fig.1. Myco-synthesis of AgNPs in the presence of dark and light conditions.

Optimization of process parameters for AgNP biosynthesis

The probable optimum levels of parameters for the generation of AgNPs were determined using OFAT, and the optimum levels of CF concentration, $AgNO_3$ concentration, and Reaction time were selected. The medium constitutions have affected the microorganism growth and their metabolite production, which are important factors for the biosynthesis of AgNPs. Our study reported that the production medium PDB was found most suitable CFC for the maximum AgNPs biosynthesis (**Fig. 2A**). To find the effect of CFC volume, the fungal culture filtrate obtained from a fungus was added at different concentrations. In the present study, maximum AgNPs were synthesized in the presence of 2.5ml of CFC volume as shown in **Fig. 2B.** Other researchers that used a fungal system to manufacture silver nanoparticles reported similar results. The color change was generated by the stimulation of Surface plasmon vibrations in metal nanoparticles. Our study reported that the maximum AgNPs were synthesized at 10 h of the incubation time at optimized conditions (**Fig. 2C**). In our study, the maximum AgNPs were biosynthesized at 1mM concentration of silver nitrate as depicted in **Fig. 2D**. According to (Rashidipour & Heydari, 2014), various concentrations of silver nitrate were optimized for the most efficient synthesis of AgNPs. Silver nitrate concentrations of 1mM encouraged fast production, but concentrations of 2mM and 3mM caused the peak to shift. During the synthesis of AgNPs, the effect of reducing agent concentration was less studied. Vigneshwaran and their colleagues reported that, AgNPs biosynthesized by using the 5% (w/v) biomass of *Aspergillus flavus*, and 1% bacterium culture *S. aureus* with $AgNO_3$ (Vigneshwaran et al., 2007). Enzymatic reduction is one of the potential paths for the production of AgNPs, hence research into its impacts is critical. The nitrate reductase enzyme, which acts as a reducing agent, is the most often used (Kalimuthu et al., 2008; Kumar et al., 2007).

Nanofabrication (2024) 9
https://doi.org/10.37819/nanofab.9.1798

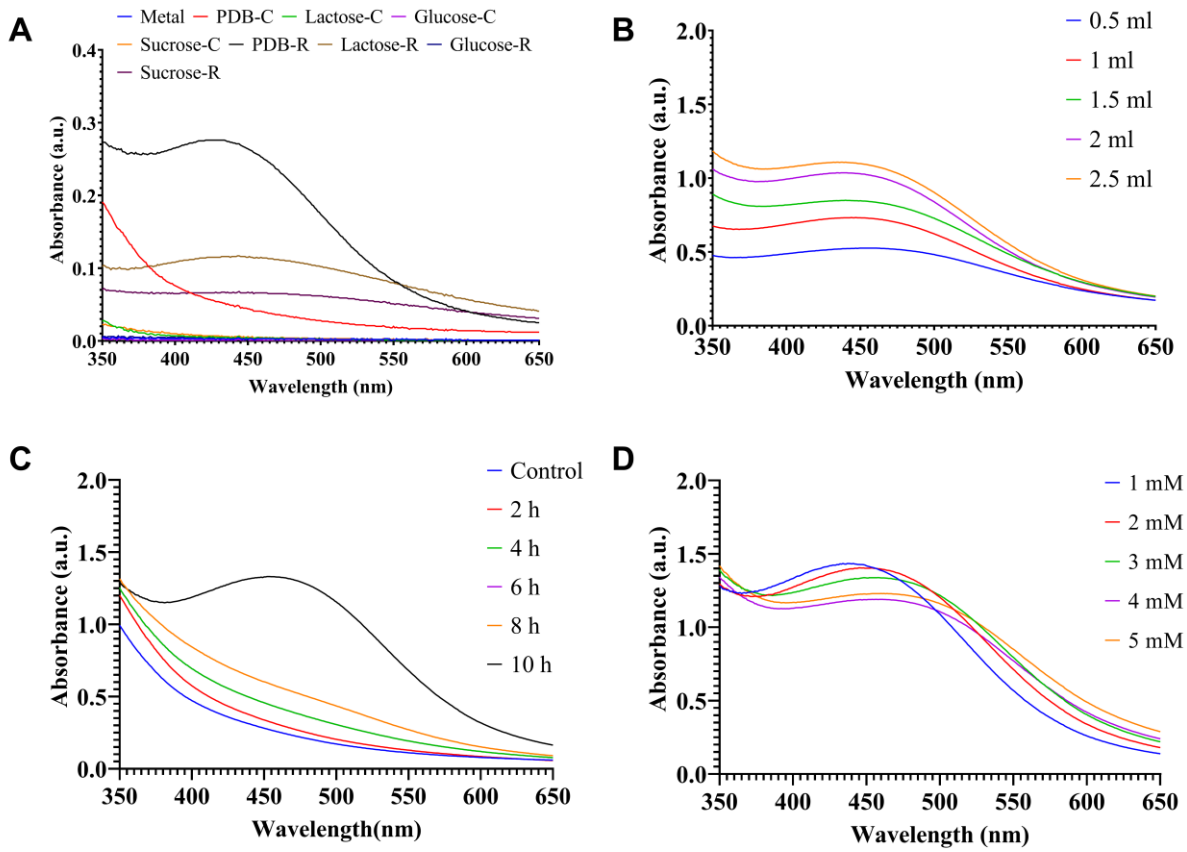

Fig. 2. OFAT optimization of AgNPs biosynthesis: (A) effect of different media CFC, (B) effect of CFC volume, (C) effect of reaction time, and (D) effect of silver nitrate concentration.

Experimental design using the CCD approach

By employing CCD design to examine the interaction effects of all three parameters (**Table 2**), the AgNPs production medium was further adjusted. With three independent variables at five levels (+, +1, 0, -1, and -), a total of 20 tests were run. **Table 4** shows that the linear model was chosen as the best match when compared to other models based on the model summary. Choose the highest-order polynomial where the model is not aliased and the additional terms are important. **Table 3** displays the observed and predicted responses. ANOVA was used to analyze the model's fitness and suitability, as shown in **Table 5**. With a calculated "F" value of 119.91 and a "p" value of < 0.0001, the ANOVA demonstrates the model's suitability (**Table 5**). In the intended space, statistical significance for the interactions between the three variables was established. The maximum AgNPs production was indicated by the linearly negative effects of all variables. The accuracy of the model was determined by the coefficient of determination R^2, which was found to be 95.74 percent, adjusted R^2, which was 94.94 percent, and predicted R^2 (92.46%) indicating a significant relationship between the experimental and anticipated response.

Table 3. Experimental matrix for process optimization through FCCCD

Runs	Factor-1	Factor-2	Factor-3	Response	
	Silver Nitrate	CFS (mL)	Reaction time (H)	Observed AgNPs	Predicted AgNPs

Nanofabrication (2024) 9
https://doi.org/10.37819/nanofab.9.1798

	(mM)			Yield (%)	Yield (%)
1	3	0.5	5.5	69.7	70.3
2	4.18	2.09	8.17	77.56	73.9
3	3	1.5	5.5	64.16	65.2
4	4.18	0.90	8.17	83.23	80.0
5	4.18	2.09	2.82	72.89	69.7
6	1	1.5	5.5	50.62	49.0
7	3	1.5	5.5	64.16	65.2
8	1.81	0.90	2.82	57.52	56.5
9	1.81	0.90	8.17	61.28	60.7
10	3	1.5	5.5	64.16	65.2
11	3	1.5	1	61	61.6
12	3	1.5	5.5	64.16	65.2
13	5	1.5	5.5	77.7	81.4
14	3	1.5	5.5	64.16	65.2
15	3	1.5	10	67.32	68.8
16	1.81	2.09	8.17	54.69	54.7
17	3	1.5	5.5	64.16	65.2
18	4.18	0.90	2.82	76.89	75.7
19	1.81	2.09	2.82	50.93	50.4
20	3	2.5	5.5	58.62	60.1

Table 4. Sequential Model Sum of Squares

Source	Sum of Squares	df	Mean Square	F-value	p-value	
Mean vs Total	85139.51	1	85139.51			
Linear vs Mean	1458.19	3	486.06	119.91	< 0.0001	**Suggested**
2FI vs Linear	3.41	3	1.14	0.2406	0.8665	
Quadratic vs 2FI	11.83	3	3.94	0.7947	0.5243	
Cubic vs Quadratic	26.09	4	6.52	1.66	0.2746	**Aliased**
Residual	23.52	6	3.92			
Total	86662.55	20	4333.13			

The lack of fit was deemed unimportant in relation to the model's validation for the current investigation. Consequently, it is possible to navigate the design space using the projected model. During the reaction, the color of

the solution changes from colorless to dark brown, which may be used to visually distinguish the formation of silver (Naveen et al., 2010). The color has altered due to the activation of surface plasmon vibration, indicating the presence of AgNPs in the solution. The surface absorption band of AgNPs was shown to be at 420 – 450nm using UV-VIS spectral analysis, which can be used for additional confirmation. The quadratic equation represents the combined influence of the model's process parameters based on the response:

AgNPs Yield (%) = 65.2455 + 9.64299*A - 3.03761*B + 2.13511*C (2)

Where, A = Silver nitrate conc., B = CFC volume, and C = Reaction time

The interactive effect of the variables in the form of a 3D surface was potted for the AgNPs Yield responses obtained in CCD design in **Fig. 3.**

Table 5. ANOVA analysis of CCD response variables

Source	Sum of Squares	df	Mean Square	F-value	p-value	
Model	1458.19	3	486.06	119.91	< 0.0001	**Significant**
A-Silver Nitrate Conc.	1269.91	1	1269.91	313.29	< 0.0001	
B-CFC	126.01	1	126.01	31.09	< 0.0001	
C-Reaction time	62.26	1	62.26	15.36	0.0012	
Residual	64.85	16	4.05			
Lack of Fit	64.85	11	5.90			
Pure Error	0.0000	5	0.0000			
Cor Total	1523.04	19				

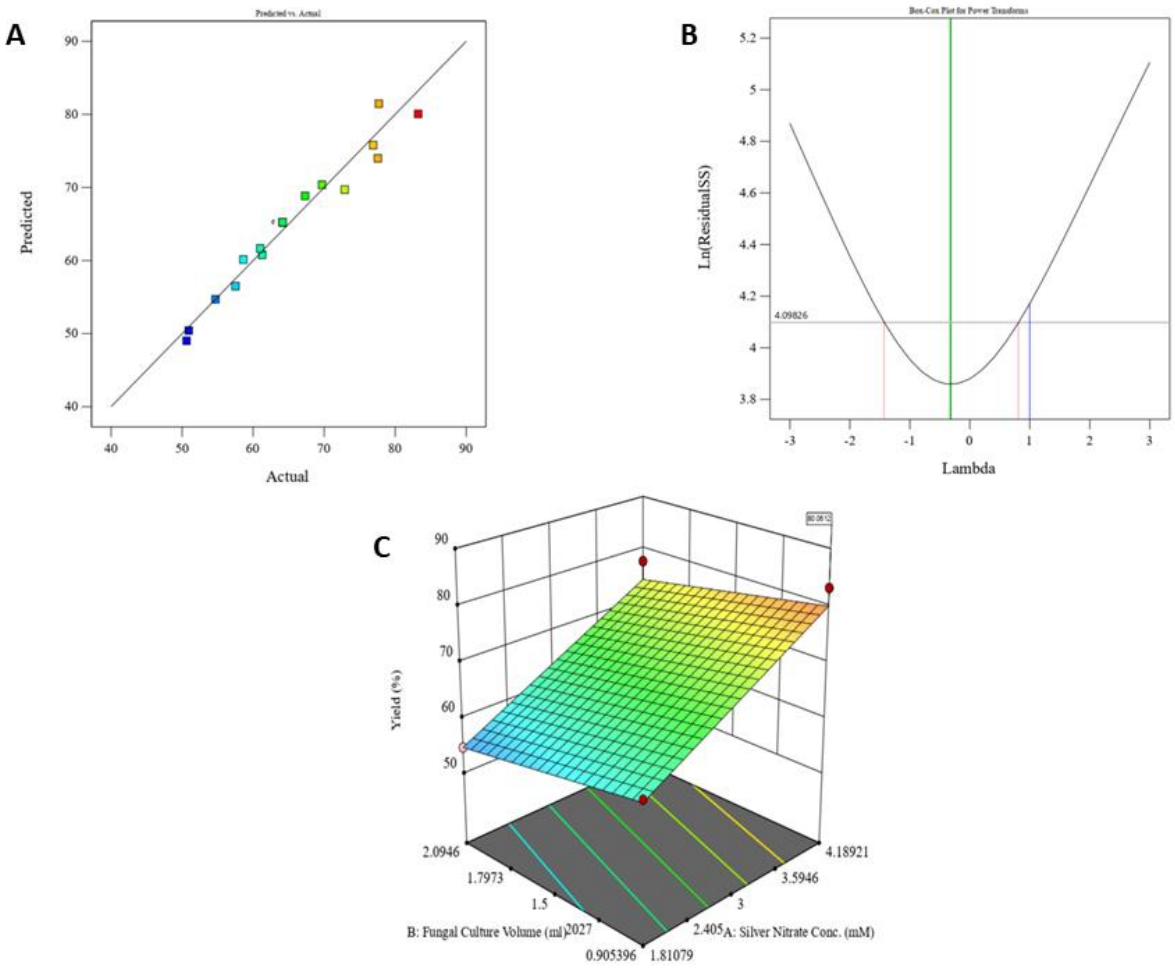

Fig. 3. Plot responses of AgNPs obtained from RSM optimization: (A) Actual vs Predicted response, (B) Box-Cox plot, and (C) 3D surface plot responses of AgNPs biosynthesis.

Validation of the experimental model

A high-intensity and narrow SPR peak at 350-420 nm was seen when the color changed from clear transparent to dark brown using UV-Visual spectroscopy The response obtained validation was found to be authenticated as the predicted response from the RSM model. Finally, it was concluded that a significant biosynthesis of AgNPs was enhanced by the statistical tool (RSM) and can be used in various fields.

Characterization of biosynthesized AgNPs

The nature of the biosynthesized AgNPs was further characterized by UV-visible spectrophotometer, FTIR spectroscopy, TEM, XRD, Zeta size, and potential. A comparative study of biosynthesized AgNPs based on previous studies has been given in **Table 6.**

UV-Visible Spectrometer

The reaction mixture became brown, suggesting the creation of silver nanoparticles. The hue of the reaction mixture evolved from light brown to dark brown as the reaction time increased. Surface Plasmon Resonance (SPR) of AgNPs was linked to the development of a band in the UV-visible spectrum at 420-430 nm, which further verified their synthesis. Electron excitation in the conductive band surrounding silver particles is seen in the SPR concept

(Neethu et al., 2018). The absorption band seen at 410 nm matches the value reported by other researchers (Elgorban et al., 2016; Ottoni et al., 2017). However, in the absence of cell-free extract, spectroscopic analysis of the silver nitrate solution revealed two bands at 240 and 280 nm.

Fourier Transform Infrared Spectroscopy (FTIR)

The functional groups associated with AgNPs synthesis were evaluated using FTIR. This interaction revealed that biomolecules are in charge of reducing silver ions. Using the FTIR spectrum, the stabilizing substance that maintains the stability and dispersion of the silver nanoparticles was discovered. Silver nanoparticles' FTIR spectra displayed five distinct peaks as shown in **Fig. 4.** Silver and bioactive chemicals, could be the cause of the creation and stability (capping material) of silver nanoparticles. The intensity at 3743.89 cm^{-1} refers to the -NH group of primary amines. The band at 1980.01 cm^{-1} represents the C-H stretch vibrational of aromatic compound. The intensity at 1637.20 cm^{-1} refers to C=C stretch. The band intensity at 1350.73 refers to the C=N stretches while 1007.89 refers to the C-C stretches. Moreover, the stretching in amide functional groups acts as on stabilization of AgNPs whereas stretching recorded in the aromatic and aliphatic amins act as reducing agents for biosynthesis of AgNPs. These findings are consistent with other researchers' observations of my synthesized AgNPs (Al-Shmgani et al., 2017; Schröfel et al., 2014). The present study was also supported by Naveen and co-workers (Naveen et al., 2010) and Raheman and their colleagues (Raheman et al., 2011).

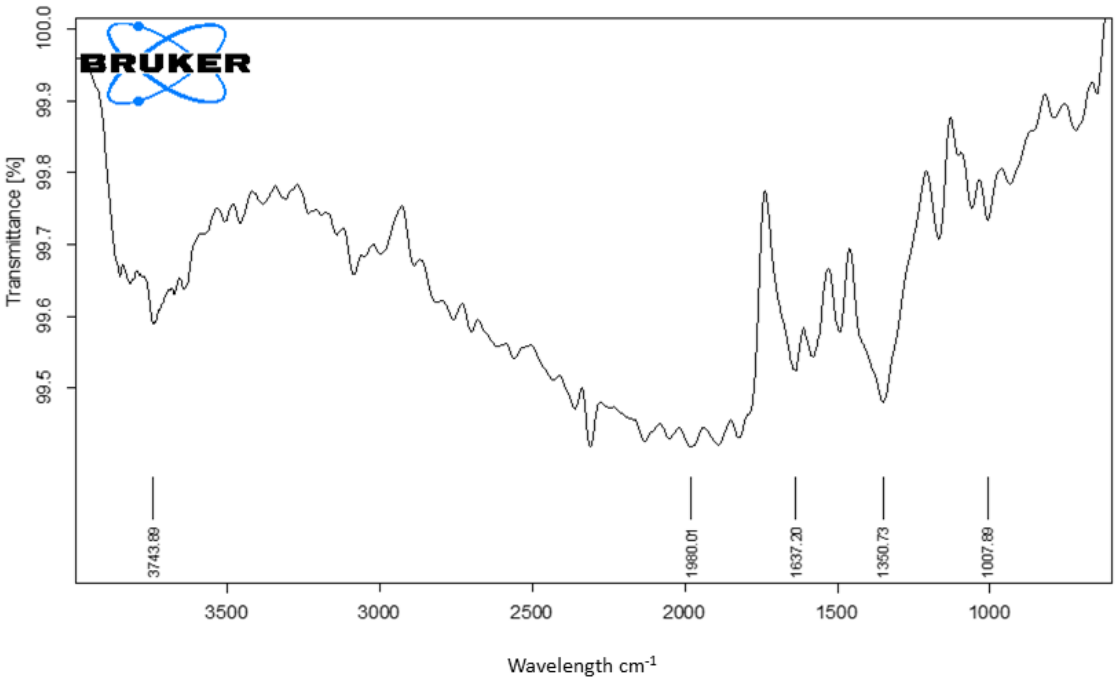

Fig. 4. FTIR Analysis of biosynthesized AgNPs from *A. flavus* GGRK1.

Zeta size and potential analysis

The zeta size analyzer revealed the biosynthesized AgNPs size of 117.4 nm (**Fig. 5A**). The negative value -14.9 mV of biosynthesized AgNPs exhibited good stability (**Fig. 5B**). The zeta potential revealed that the surface charge and physical stability of nanosuspensions (Jiang et al., 2009). According to Ferreyra Maillard and co-workers, zeta potential has an evaluating capability of interaction between antimicrobial compounds and bacteria (Ferreyra Maillard et al., 2021). A similar study reported by Gecer and Erenler in 2023 (Gecer & Erenler, 2023).

Nanofabrication (2024) 9
https://doi.org/10.37819/nanofab.9.1798

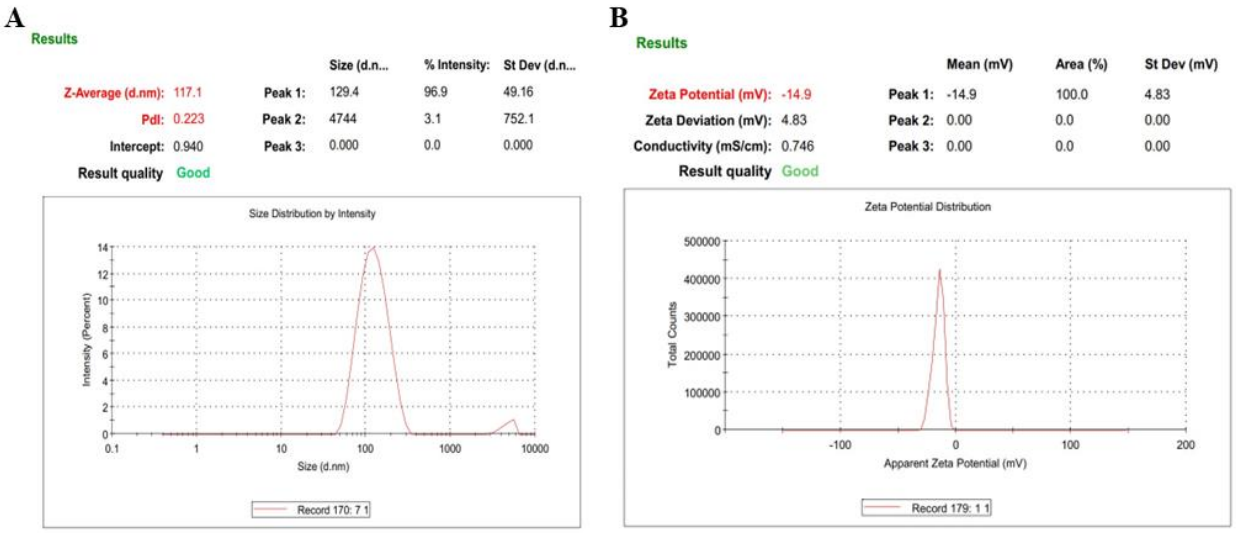

Fig. 5. Zeta size (A) and zeta potential (B) of biosynthesized AgNPs.

X-ray diffraction analysis

The crystalline quality of biosynthesized AgNPs was determined by different diffraction peaks in the XRD study, as depicted in **Fig. 6**. The XRD spectra revealed 09 sharp peaks at 2θ positions of 26.58°, 27.7°, 32.16°, 38.02°, 46.12°, 50.66°, 54.78°, 57.42° and 59.98° in the XRD graph, that matched to diffraction from silver planes with FCC lattice (JCPDS card No. 04–0783) (**Fig. 6**). This pattern confirm that the biosynthesized AgNPs had a nanoscale size and crystalline nature (Rose et al., 2019). The findings are consistent with previous investigations that reported equal diffraction peaks for silver nanoparticles (Venkatesan et al., 2014).

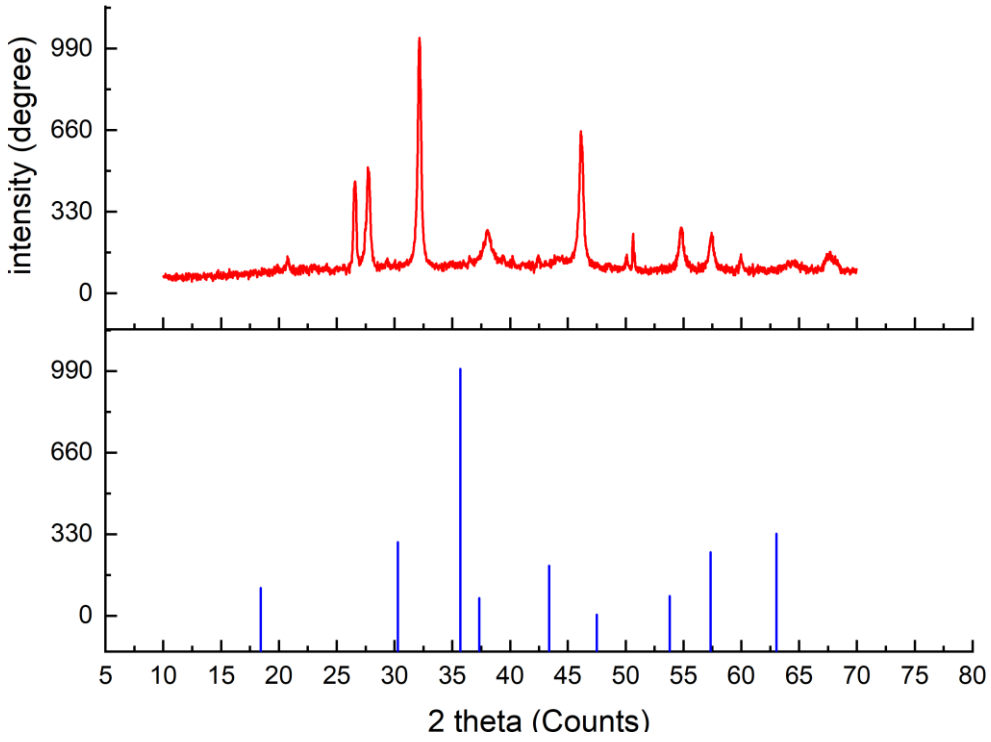

Fig. 6. XRD analysis of biosynthesized AgNPs from *A. flavus* GGRK1.

Transmission electron microscopy analysis

The size, surface morphology and distribution of the biosynthesized AgNPs are shown in **Fig. 7**. The TEM image of biosynthesized AgNPs revealed the oval to spherical shaped and polydispersed nature of the NPs. Additionally, the size ranged from 15 to 55 nm, with an average particle size of 20.5 nm and a PDI of 0.33, which indicates the polydispersity of biosynthesized AgNPs (**Fig. 7B**). The histogram analysis of AgNPs was given in the **Fig. 7B**. The average homogeneity of the particles inside the solution is determined using PDI, which spans from 0 to 1. A PDI value of more than 0.1 indicates a polydispersed nature; less than 0.1 indicates a monodispersed nature (Rudrappa et al., 2022). AgNPs from *Aspergillus sydowii* had comparable polydispersity and size distribution, with particle sizes ranging from 1 to 21 nm (Wang et al., 2021).

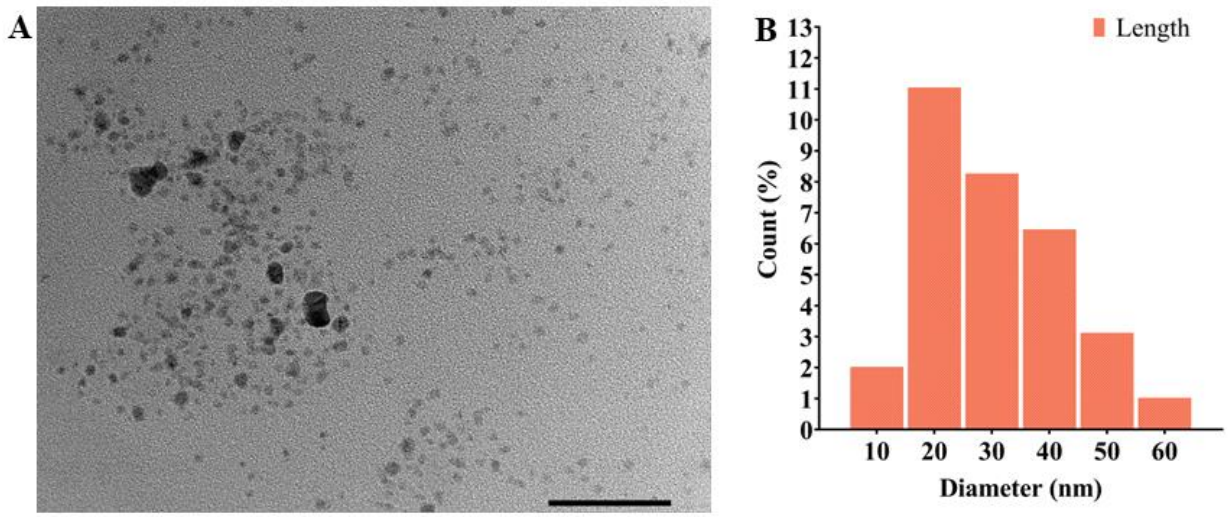

Fig. 7. TEM analysis of biosynthesized AgNPs from *A. flavus* GGRK1; A) TEM Image of silver nanoparticles, B) Histogram showing size distribution.

Table 6: A comparative analysis of the greener synthesis of AgNPs and their characteristics and features were previously reported and compared with the present study

S. No.	Microorganisms	Optimization Process	Synthesis conditions	Characterization				References
				XRD analysis	Size	PDI	Zeta potential	
1	*Aspergillus sydowii*	OFAT	Temperature of 50 °C, pH 8.0, and substrate conc. of 1.5 mM	Crystalline cubic feature	12 nm	-	-	(Wang et al., 2021)
2	*Aspergillus melleus* SSS-10	OFAT	Colour changed after 24 hrs of reaction	Crystalline nature	87.3 nm	-	− 19.6 mV	(Skanda et al., 2022)
3	*Penicillium* sp. 8L2	Rotatable Central Composite	Optimized condition	Highly crystalline nature	2 and 9 nm	-	-	(Muñoz et al., 2022)

		Design		followed the JCPS pattern				
4	*Letendraea* sp. WZ07	OFAT	At ordinary reaction mixture and temperature	face-centered cubic in crystalline nature	33.8 nm	-	-	(Qiao et al., 2022)
5	*Sclerotinia sclerotiorum* MTCC 8785	OFAT	At pH 7, 28 °C under dark conditions	-	10-50 nm and 40-50 nm	-	-	(Saxena & Ayushi, 2023)
6	*Humicola* sp.	OFAT	At 1 mM $AgNO_3$, 50 °C and pH 9 for 96 h under shaking condition	face-centered cubic silver NPs	5-25 nm	-	-	(Syed et al., 2013)
7	*Thermomyces lanuginosus*	Placket Berman model	Optimized conditions	7–24 nm diameter in crystalline size	5-35 nm	-	-	(Zainab et al., 2023)
8	*Aspergillus flavus* GGRK1	Central composite design	At $AgNO_3$ conc. of 4.189 mM, CFC 0.905 mL, and reaction time 8.17 h.	XRD graph, that matched diffraction from silver planes with FCC lattice (JCPDS card No. 04–0783)	20.5 nm	0.33	− 14.9 mV	Present report

Determination of antibacterial activity of biosynthesized AgNPs

The biosynthesized AgNPs showed substantial antibacterial efficacy against tested microorganisms (**Fig. 8** and **Table 7**). The bacteria such as *B. subtilis* MTCC 121, *S. aureus* MTCC 96, and *E coli* MTCC 443 showed resistances at 50 µl/ml conc. of AgNPs. While the AgNPs concentration of 50 µl/ml showed sensitivity against *P. aeruginosa* MTCC 424. Hence as shown in **Table 6**, 75 µl/ml concentration of AgNPs was determined as Minimum inhibitory concentration (MIC) against *B. subtilis* MTCtC 121, *S. aureus* MTCC 96, and *E coli* MTCC 443 with inhibition zones measuring 11 mm, 16 mm, and 07 mm, respectively. In the case of *P. aeruginosa* MTCC 424, MIC was found at 50 µl/ml of AgNPs with a 13 mm zone of inhibition. Interestingly, the obtained results are somehow similar to those reported by the biosynthesized AgNPs by *A. terreus* NRRL265 CFF (Othman et al., 2021) and greater than the *A. fumigatus* synthesized AgNPs (Othman et al., 2019). In the present study, better and more significant antibacterial activity was obtained as compared to previous study reported. The antibacterial mechanism of AgNPs assumed that formation of holes in the bacterial cell wall (Sondi & Salopek-Sondi, 2004). Another possible mechanism of antibacterial activity, the AgNPs could bind with the cell wall or cell membrane and disfunction the respiratory process of the bacterial cell (Rai et al., 2009). A study reported by Maliszewska and Sadowski in 2009 they concluded that the silver nanoparticles inhibited the development of bacteria such as *Bacillus cereus*, *Staphylococcus aureus*, *E. coli*, and *Pseudomonas aeruginosa* (Maliszewska & Sadowski, 2009). Similarly,

another study revealed the antimicrobial efficacy of *Aspergillus clavatus* synthesized silver nanoparticles against *Candida albicans*, *Pseudomonas fluorescens*, and *E. coli* (Omran et al., 2018).

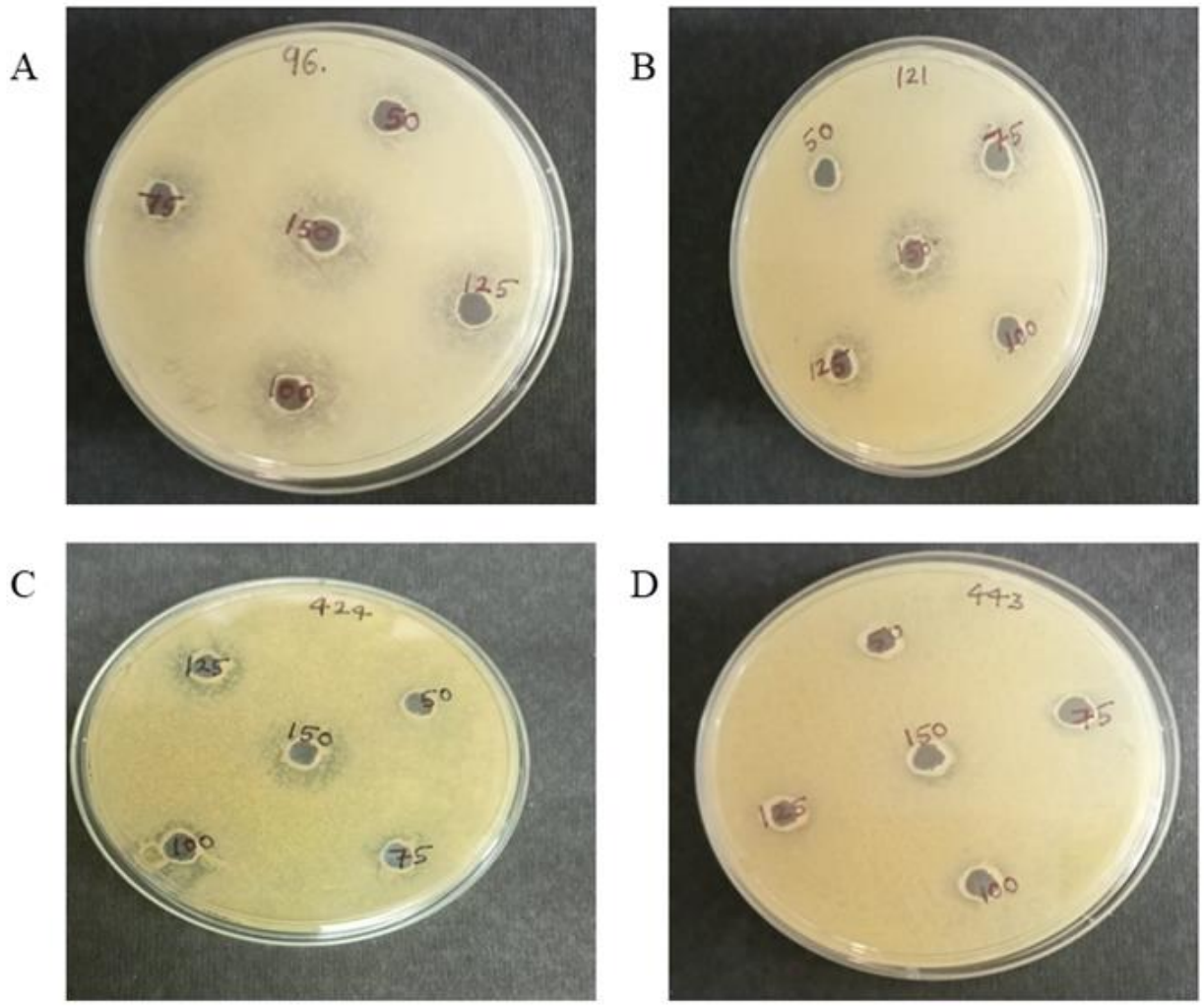

Fig. 8. Antibacterial efficacy of synthesized AgNPs; A) *S. aureus* MTCC 96, B) *B. subtilis* MTCC 121, C) *Pseudomonas aeruginosa* MTCC 424, and D) *E. coli* MTCC 443.

Table 7: The antibacterial activity of biosynthesized AgNPs using *A. Flavus* GGRK1 Cell-free culture filtrate against gram-positive and gram-negative bacteria

AgNPs concentration (µl/ml)	**Zone of Inhibition (mm)**			
	***Bacillus subtilis* MTCC 121**	***Pseudomonas aeruginosa* MTCC 424**	***E. coli* MTCC 443**	***Staphylococcus aureus* MTCC 96**
50	**R**	13	**R**	**R**
75	11	14	07	16
100	13	14	09	17

125	14	13	12	18
150	**18**	**18**	**14**	**20**

Conclusion and Future Perspectives

The study aimed to optimize the maximum biosynthesis of silver nanoparticles using both conventional (OFAT) and statistical (RSM) approaches. In the OFAT approach, various physio-chemical factors including media, AgNO3 concentration, cell-free culture filtrate volume, temperature, pH, reaction time, and light conditions were optimized. These parameters were then further optimized for maximum biosynthesis of silver nanoparticles. Cell-free culture filtrate of *A. flavus* GGRK1, used as a green approach to the biosynthesis of AgNPs has been established. A statistical optimization process has been developed for the myco-synthesis of AgNPs. The anti-bacterial efficacy of the produced AgNPs has also been investigated. Ultimately, it was concluded that the statistical tool (RSM) greatly enhanced the biosynthesis of silver nanoparticles (AgNPs) and holds potential for various applications across different fields such as medicinal agents, food preservatives, and environmental pollutants.

Acknowledgment

The authors are grateful to DST–FIST laboratory of Department of Microbiology, M. D. University, Rohtak for providing research facilities that allowed them to complete this study. We are also appreciative to the Departments of Biotechnology, UIET, M. D. University, Rohtak, and Physics, M. D. University, Rohtak, for providing FT-IR and XRD facilities, respectively.

Conflict of interest

The authors have no conflict of interest.

References

Al-Shmgani, H. S. A., Mohammed, W. H., Sulaiman, G. M., & Saadoon, A. H. (2017). Biosynthesis of silver nanoparticles from Catharanthus roseus leaf extract and assessing their antioxidant, antimicrobial, and wound-healing activities. *Artificial Cells, Nanomedicine and Biotechnology*, *45*(6), 1234–1240. https://doi.org/10.1080/21691401.2016.1220950

Balavandy, S. K., Shameli, K., Biak, D. R. B. A., & Abidin, Z. Z. (2014). Stirring time effect of silver nanoparticles prepared in glutathione mediated by green method. *Chemistry Central Journal*, *8*(1). https://doi.org/10.1186/1752-153X-8-11

Bhainsa, K. C., & D'Souza, S. F. (2006). Extracellular biosynthesis of silver nanoparticles using the fungus Aspergillus fumigatus. *Colloids and Surfaces B: Biointerfaces*, *47*(2), 160–164. https://doi.org/10.1016/j.colsurfb.2005.11.026

Chauhan, A., Anand, J., Parkash, V., & Rai, N. (2023). Biogenic synthesis: a sustainable approach for nanoparticle synthesis mediated by fungi. In *Inorganic and Nano-Metal Chemistry* (Vol. 53, Issue 5, pp. 460–473). Taylor and Francis Ltd. https://doi.org/10.1080/24701556.2021.2025078

Dhillon, G. S., Brar, S. K., Kaur, S., & Verma, M. (2012). Green approach for nanoparticle biosynthesis by fungi: Current trends and applications. In *Critical Reviews in Biotechnology* (Vol. 32, Issue 1, pp. 49–73). https://doi.org/10.3109/07388551.2010.550568

Elgorban, A. M., Al-Rahmah, A. N., Sayed, S. R., Hirad, A., Mostafa, A. A. F., & Bahkali, A. H. (2016). Antimicrobial activity and green synthesis of silver nanoparticles using Trichoderma viride. *Biotechnology and Biotechnological Equipment*, *30*(2), 299–304. https://doi.org/10.1080/13102818.2015.1133255

Elshafei, A. M., Othman, A. M., Elsayed, M. A., Al-Balakocy, N. G., & Hassan, M. M. (2021). Green synthesis of

silver nanoparticles using Aspergillus oryzae NRRL447 exogenous proteins: Optimization via central composite design, characterization and biological applications. *Environmental Nanotechnology, Monitoring, and Management*, *16*, 100553. https://doi.org/10.1016/j.enmm.2021.100553

Farrag, H. M. M., Mostafa, F. A. A. M., Mohamed, M. E., & Huseein, E. A. M. (2020). Green biosynthesis of silver nanoparticles by Aspergillus niger and its antiamoebic effect against Allovahlkampfia spelaea trophozoite and cyst. *Experimental Parasitology*, *219*, 108031. https://doi.org/10.1016/j.exppara.2020.108031

Ferreyra Maillard, A. P. V., Espeche, J. C., Maturana, P., Cutro, A. C., & Hollmann, A. (2021). Zeta potential beyond materials science: Applications to bacterial systems and to the development of novel antimicrobials. In *Biochimica et Biophysica Acta - Biomembranes* (Vol. 1863, Issue 6). https://doi.org/10.1016/j.bbamem.2021.183597

Gecer, E. N., & Erenler, R. (2023). Biogenic synthesis of silver nanoparticles using Echium vulgare: Characterisation, quantitative analysis of bioactive compounds, antioxidant activity, and catalytic degradation. *Journal of the Indian Chemical Society*, *100*(5), 101003. https://doi.org/10.1016/j.jics.2023.101003

Hulkoti, N. I., & Taranath, T. C. (2014). Biosynthesis of nanoparticles using microbes-A review. In *Colloids and Surfaces B: Biointerfaces* (Vol. 121, pp. 474–483). https://doi.org/10.1016/j.colsurfb.2014.05.027

Ifijen, I. H., Maliki, M., & Anegbe, B. (2022). Synthesis, photocatalytic degradation and antibacterial properties of selenium or silver doped zinc oxide nanoparticles: A detailed review. In *OpenNano* (Vol. 8). https://doi.org/10.1016/j.onano.2022.100082

Jiang, J., Oberdörster, G., & Biswas, P. (2009). Characterization of size, surface charge, and agglomeration state of nanoparticle dispersions for toxicological studies. *Journal of Nanoparticle Research*, *11*(1), 77–89. https://doi.org/10.1007/S11051-008-9446-4

Kalimuthu, K., Suresh Babu, R., Venkataraman, D., Bilal, M., & Gurunathan, S. (2008). Biosynthesis of silver nanocrystals by Bacillus licheniformis. *Colloids and Surfaces B: Biointerfaces*, *65*(1), 150–153. https://doi.org/10.1016/j.colsurfb.2008.02.018

Kapoor, R. T., Salvadori, M. R., Rafatullah, M., Siddiqui, M. R., Khan, M. A., & Alshareef, S. A. (2021). Exploration of Microbial Factories for Synthesis of Nanoparticles – A Sustainable Approach for Bioremediation of Environmental Contaminants. In *Frontiers in Microbiology* (Vol. 12). Frontiers Media S.A. https://doi.org/10.3389/fmicb.2021.658294

Khandel, P., & Shahi, S. K. (2018). Mycogenic nanoparticles and their bio-prospective applications: current status and future challenges. In *Journal of Nanostructure in Chemistry* (Vol. 8, Issue 4, pp. 369–391). Springer Medizin. https://doi.org/10.1007/s40097-018-0285-2

Kumar, S. A., Abyaneh, M. K., Gosavi, S. W., Kulkarni, S. K., Pasricha, R., Ahmad, A., & Khan, M. I. (2007). Nitrate reductase-mediated synthesis of silver nanoparticles from AgNO 3. *Biotechnology Letters*, *29*(3), 439–445. https://doi.org/10.1007/s10529-006-9256-7

Lee, H. J., Lee, G., Jang, N. R., Yun, J. H., Song, J. Y., & Kim, B. S. (2011). Biological synthesis of copper nanoparticles using plant extract. *Technical Proceedings of the 2011 NSTI Nanotechnology Conference and Expo, NSTI-Nanotech 2011*, *1*, 371–374.

Ma, L., Su, W., Liu, J. X., Zeng, X. X., Huang, Z., Li, W., Liu, Z. C., & Tang, J. X. (2017). Optimization for extracellular biosynthesis of silver nanoparticles by Penicillium aculeatum Su1 and their antimicrobial activity and cytotoxic effect compared with silver ions. *Materials Science and Engineering C*, *77*, 963–971. https://doi.org/10.1016/j.msec.2017.03.294

Majeed, S., Abdullah, M. S. bin, Nanda, A., & Ansari, M. T. (2016). In vitro study of the antibacterial and anticancer activities of silver nanoparticles synthesized from Penicillium brevicompactum (MTCC-1999). *Journal of Taibah University for Science*, *10*(4), 614–620. https://doi.org/10.1016/j.jtusci.2016.02.010

Maliszewska, I., & Sadowski, Z. (2009). Synthesis and antibacterial activity of silver nanoparticles. *Journal of Physics: Conference Series*, *146*. https://doi.org/10.1088/1742-6596/146/1/012024

Mansouri, S. S., & Ghader, S. (2009). Experimental study on the effect of different parameters on the size and shape of triangular silver nanoparticles prepared by a simple and rapid method in an aqueous solution. *Arabian Journal of Chemistry*, *2*(1), 47–53. https://doi.org/10.1016/j.arabjc.2009.07.004

Mostafa, F. (2017). Biosynthesis of Silver Nanoparticles by Pathogenic and Nonpathogenic Strains of Fusarium oxysporum f. sp. lycopersici. *Egyptian Journal of Botany*, *57*(2), 345–350. https://doi.org/10.21608/ejbo.2017.789.1048

Muñoz, A. J., Espínola, F., Ruiz, E., Cuartero, M., & Castro, E. (2022). Biotechnological use of the ubiquitous fungus Penicillium sp. 8L2: Biosorption of Ag(I) and synthesis of silver nanoparticles. *Journal of Environmental Management*, *316*, 115281. https://doi.org/10.1016/j.jenvman.2022.115281

Naveen, N., Kumar, R., Balaji, S., Uma, T. S., Natrajan, T. S., & Sehgal, P. K. (2010). Synthesis of nonwoven nanofibers by electrospinning - A promising biomaterial for tissue engineering and drug delivery. *Advanced Engineering Materials*, *12*(8). https://doi.org/10.1002/ADEM.200980067

Nayak, R. R., Pradhan, N., Behera, D., Pradhan, K. M., Mishra, S., Sukla, L. B., & Mishra, B. K. (2011). Green synthesis of silver nanoparticle by Penicillium purpurogenum NPMF: The process and optimization. *Journal of Nanoparticle Research*, *13*(8), 3129–3137. https://doi.org/10.1007/s11051-010-0208-8

Neethu, S., Midhun, S. J., Sunil, M. A., Soumya, S., Radhakrishnan, E. K., & Jyothis, M. (2018). Efficient visible-light-induced synthesis of silver nanoparticles by Penicillium polonium ARA 10 isolated from Chetomorpha antenna and its antibacterial efficacy against Salmonella enterica serovar Typhimurium. *Journal of Photochemistry and Photobiology B: Biology*, *180*, 175–185. https://doi.org/10.1016/j.jphotobiol.2018.02.005

Omran, B. A., Nassar, H. N., Fatthallah, N. A., Hamdy, A., El-Shatoury, E. H., & El-Gendy, N. S. (2018). Characterization and antimicrobial activity of silver nanoparticles mycosynthesized by Aspergillus brasiliensis. *Journal of Applied Microbiology*, *125*(2), 370–382. https://doi.org/10.1111/jam.13776

Othman, A. M., Elsayed, M. A., Al-Balakocy, N. G., Hassan, M. M., & Elshafei, A. M. (2019). Biosynthesis and characterization of silver nanoparticles induced by fungal proteins and their application in different biological activities. *Journal of Genetic Engineering and Biotechnology*, *17*(1), 1–13. https://doi.org/10.1186/s43141-019-0008-1

Othman, A. M., Elsayed, M. A., Al-Balakocy, N. G., Hassan, M. M., & Elshafei, A. M. (2021). Biosynthesized silver nanoparticles by Aspergillus terreus NRRL265 for imparting durable antimicrobial finishing to polyester cotton blended fabrics: Statistical optimization, characterization, and antitumor activity evaluation. *Biocatalysis and Agricultural Biotechnology*, *31*, 101908. https://doi.org/10.1016/j.bcab.2021.101908

Ottoni, C. A., Simões, M. F., Fernandes, S., dos Santos, J. G., da Silva, E. S., de Souza, R. F. B., & Maiorano, A. E. (2017). Screening of filamentous fungi for antimicrobial silver nanoparticles synthesis. *AMB Express*, *7*(1). https://doi.org/10.1186/S13568-017-0332-2

Qiao, Z. P., Wang, M. Y., Liu, J. F., & Wang, Q. Z. (2022). Green synthesis of silver nanoparticles using a novel endophytic fungus Letendraea sp. WZ07: Characterization and evaluation of antioxidant, antibacterial, and catalytic activities (3-in-1 system). *Inorganic Chemistry Communications*, *138*, 109301. https://doi.org/10.1016/j.inoche.2022.109301

Raheman, F., Raheman, F., Deshmukh, S., Ingle, A., Gade, A., & Rai, M. (2011). Silver nanoparticles: novel antimicrobial agent synthesized from an endophytic fungus Pestalotia sp. isolated from leaves of Syzygium cumini (L). *Researchgate.NetF Raheman, S Deshmukh, A Ingle, A Gade, M RaiNano Biomed Eng, 2011•researchgate.Net*, *2011*(3), 174–178. https://doi.org/10.5101/nbe.v3i3.p174-178

Rai, M., Yadav, A., & Gade, A. (2009). Silver nanoparticles as a new generation of antimicrobials. In *Biotechnology Advances* (Vol. 27, Issue 1, pp. 76–83). https://doi.org/10.1016/j.biotechadv.2008.09.002

Rashidipour, M., & Heydari, R. (2014). Biosynthesis of silver nanoparticles using extract of olive leaf: synthesis and in vitro cytotoxic effect on MCF-7 cells. *Journal of Nanostructure in Chemistry*, *4*(3). https://doi.org/10.1007/S40097-014-0112-3

Rose, G. K., Soni, R., Rishi, P., & Soni, S. K. (2019). Optimization of the biological synthesis of silver nanoparticles using Penicillium oxalicum GRS-1 and their antimicrobial effects against common food-borne pathogens. *Green Processing and Synthesis*, *8*(1), 144–156. https://doi.org/10.1515/gps-2018-0042

Rudrappa, M., Rudayni, H. A., Assiri, R. A., Bepari, A., Basavarajappa, D. S., Nagaraja, S. K., Chakraborty, B., Swamy, P. S., Agadi, S. N., Niazi, S. K., & Nayaka, S. (2022). Plumeria alba-Mediated Green Synthesis of Silver Nanoparticles Exhibits Antimicrobial Effect and Anti-Oncogenic Activity against Glioblastoma U118 MG Cancer Cell Line. *Nanomaterials*, *12*(3). https://doi.org/10.3390/nano12030493

Saxena, J., & Ayushi, K. M. (2023). Evaluation of Sclerotinia sclerotiorum MTCC 8785 as a biological agent for the synthesis of silver nanoparticles and assessment of their antifungal potential against Trichoderma harzianum MTCC 801. *Environmental Research*, *216*, 114752. https://doi.org/10.1016/j.envres.2022.114752

Schröfel, A., Kratošová, G., Šafařík, I., Šafaříková, M., Raška, I., & Shor, L. M. (2014). Applications of biosynthesized metallic nanoparticles - A review. In *Acta Biomaterialia* (Vol. 10, Issue 10, pp. 4023–4042). https://doi.org/10.1016/j.actbio.2014.05.022

Sheikh, H., & Awad, M. F. (2022). Biogenesis of nanoparticles with inhibitory effects on aflatoxin B1 production by Aspergillus flavus. *Electronic Journal of Biotechnology*, *60*, 26–35. https://doi.org/10.1016/j.ejbt.2022.09.003

Shinde, M. U., Patwekar, M., Patwekar, F., Bajaber, M. A., Medikeri, A., Mohammad, F. S., Mukim, M., Soni, S., Mallick, J., & Jawaid, T. (2022). Nanomaterials: A Potential Hope for Life Sciences from Bench to Bedside. In *Journal of Nanomaterials* (Vol. 2022). https://doi.org/10.1155/2022/5968131

Singh, J., Dutta, T., Kim, K. H., Rawat, M., Samddar, P., & Kumar, P. (2018). 'Green' synthesis of metals and their oxide nanoparticles: Applications for environmental remediation. *Journal of Nanobiotechnology*, *16*(1). https://doi.org/10.1186/S12951-018-0408-4

Singh, R., Shedbalkar, U. U., Wadhwani, S. A., & Chopade, B. A. (2015). Bacteriagenic silver nanoparticles: synthesis, mechanism, and applications. *Applied Microbiology and Biotechnology*, *99*(11), 4579–4593. https://doi.org/10.1007/S00253-015-6622-1

Skanda, S., Bharadwaj, P. S. J., Datta Darshan, V. M., Sivaramakrishnan, V., & Vijayakumar, B. S. (2022). Proficient mycogenic synthesis of silver nanoparticles by soil derived fungus Aspergillus melleus SSS-10 with cytotoxic and antibacterial potency. *Journal of Microbiological Methods*, *199*, 106517. https://doi.org/10.1016/j.mimet.2022.106517

Sondi, I., & Salopek-Sondi, B. (2004). Silver nanoparticles as antimicrobial agent: A case study on E. coli as a model for Gram-negative bacteria. *Journal of Colloid and Interface Science*, *275*(1), 177–182. https://doi.org/10.1016/j.jcis.2004.02.012

Sreenivasa, N., Meghashyama, B. P., Pallavi, S. S., Bidhayak, C., Dattatraya, A., Muthuraj, R., Shashiraj, K. N., Halaswamy, H., Dhanyakumara, S. B., & Vaishnavi, M. D. (2021). Biogenic synthesis of silver nanoparticles using Paenibacillus sp. in-vitro and their antibacterial, anticancer activity assessment against human colon tumour cell line. *Journal of Environmental Biology*, *42*(1), 118–127. https://doi.org/10.22438/JEB/42/1/MRN-1401

Sulaiman, G. M., Hussien, H. T., & Saleem, M. M. N. M. (2015). Biosynthesis of silver nanoparticles synthesized by Aspergillus flavus and their antioxidant, antimicrobial and cytotoxicity properties. *Bulletin of Materials Science*, *38*(3), 639–644. https://doi.org/10.1007/s12034-015-0905-0

Syed, A., Saraswati, S., Kundu, G. C., & Ahmad, A. (2013). Biological synthesis of silver nanoparticles using the fungus Humicola sp. And evaluation of their cytoxicity using normal and cancer cell lines. *Spectrochimica Acta - Part A: Molecular and Biomolecular Spectroscopy*, *114*, 144–147.

https://doi.org/10.1016/j.saa.2013.05.030

Thomas, S., Nair, S. K., Jamal, E. M. A., Al-Harthi, S. H., Varma, M. R., & Anantharaman, M. R. (2008). Size-dependent surface plasmon resonance in silver silica nanocomposites. *Nanotechnology*, *19*(7). https://doi.org/10.1088/0957-4484/19/7/075710

Venkatesan, B., Subramanian, V., Tumala, A., & Vellaichamy, E. (2014). Rapid synthesis of biocompatible silver nanoparticles using aqueous extract of Rosa damascena petals and evaluation of their anticancer activity. *Asian Pacific Journal of Tropical Medicine*, *7*(S1), S294–S300. https://doi.org/10.1016/S1995-7645(14)60249-2

Vigneshwaran, N., Ashtaputre, N. M., Varadarajan, P. V., Nachane, R. P., Paralikar, K. M., & Balasubramanya, R. H. (2007). Biological synthesis of silver nanoparticles using the fungus Aspergillus flavus. *Materials Letters*, *61*(6), 1413–1418. https://doi.org/10.1016/j.matlet.2006.07.042

Wang, D., Xue, B., Wang, L., Zhang, Y., Liu, L., & Zhou, Y. (2021). Fungus-mediated green synthesis of nano-silver using Aspergillus sydowii and its antifungal/antiproliferative activities. *Scientific Reports*, *11*(1). https://doi.org/10.1038/s41598-021-89854-5

Wei, S., Wang, Y., Tang, Z., Hu, J., Su, R., Lin, J., Zhou, T., Guo, H., Wang, N., & Xu, R. (2020). A size-controlled green synthesis of silver nanoparticles by using the berry extract ofSea Buckthornand their biological activities. *New Journal of Chemistry*, *44*(22), 9304–9312. https://doi.org/10.1039/d0nj01335h

Zainab, S., Jadoon, M., Sikandar, S., & Ali, N. (2023). Thermomyces lanuginosus: A prospective thermophilic fungus for green synthesis and stabilization of BioAgNPs through glucoamylase. *Materials Chemistry and Physics*, *297*, 127442. https://doi.org/10.1016/j.matchemphys.2023.127442